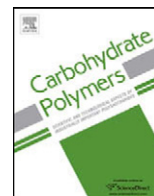




Since January 2020 Elsevier has created a COVID-19 resource centre with free information in English and Mandarin on the novel coronavirus COVID-19. The COVID-19 resource centre is hosted on Elsevier Connect, the company's public news and information website.

Elsevier hereby grants permission to make all its COVID-19-related research that is available on the COVID-19 resource centre - including this research content - immediately available in PubMed Central and other publicly funded repositories, such as the WHO COVID database with rights for unrestricted research re-use and analyses in any form or by any means with acknowledgement of the original source. These permissions are granted for free by Elsevier for as long as the COVID-19 resource centre remains active.



## Cellulose–polymer–Ag nanocomposite fibers for antibacterial fabrics/skin scaffolds

Gownolla Malegowd Raghavendra<sup>a</sup>, Tippabattini Jayaramudu<sup>a</sup>, Kokkarachedu Varaprasad<sup>b,\*</sup>, Rotimi Sadiku<sup>b</sup>, S. Sinha Ray<sup>c</sup>, Konduru Mohana Raju<sup>a</sup>

<sup>a</sup> Synthetic Polymer Laboratory, Department of Polymer Science & Technology, Sri Krishnadevaraya University, Anantapur 515003, India

<sup>b</sup> Department of Polymer Technology, Tshwane University of Technology, CSIR Campus, Building 14D, Private Bag X025, Lynwood Ridge 0040, Pretoria, South Africa

<sup>c</sup> DST/CSIR Nanotechnology Innovation Centre, National Centre for Nano-Structured Materials, Council for Scientific and Industrial Research, Pretoria 0001, South Africa

### ARTICLE INFO

#### Article history:

Received 25 November 2012

Accepted 14 December 2012

Available online 25 December 2012

#### Keywords:

Gum acacia

Gaur gum

Carbohydrates

Silver nanoparticles

Cellulose fibers

Antibacterial activity

### ABSTRACT

Natural carbohydrates (polysaccharides): gum acacia (GA) and gaur gum (GG) were employed in dilute solutions: 0.3%, 0.5% and 0.7% (w/v), as effective reductants for the green synthesis of silver nanoparticles (AgNPs) from AgNO<sub>3</sub>. The formed AgNPs were impregnated into cellulose fibers after confirming their formation by utilizing ultraviolet–visible (UV–vis) spectral studies, Fourier transforms infrared (FTIR) and transmission electron microscopy (TEM). The surface morphology of the developed cellulose–silver nanocomposite fibers (CSNCFs) were examined with scanning electron microscope–energy dispersive spectroscopy (SEM–EDS). The thermal stability and mechanical properties of the CSNCFs were found to be better than cellulose fibers alone. The antibacterial activity of the nanocomposites was studied by inhibition zone method against *Escherichia coli*, which suggested that the developed CSNCFs can function effectively as anti-microbial agents. Hence, the developed CSNCFs can effectively used for tissue scaffolding.

© 2012 Elsevier Ltd. All rights reserved.

### 1. Introduction

In the medical field, medical fabrics are gaining significant importance as health care materials especially in the past two decades. Essentially, these public health materials should provide adequate barriers against highly communicable bacteria and viruses. The spread of HIV, hepatitis viruses, severe acute respiratory syndrome (SARS), etc., by contacting with contaminated materials, has created increased pressure for the protection of the personnel with functional clothing. In the surgical zone, a lot of priority has been given to the protection of the surgical team from the patient's infectious blood and other body fluids and vice versa. Therefore, surgical fabrics should possess more antimicrobial properties (Vaideki, Jayakumar, Rajendran, & Thilagavathi, 2008; Mucha, Hoter, & Swerev, 2002). The cellulose fiber skin scaffolds contain cellulose, a homopolymer of β-D-glucopyranose units linked together by (1→4)-glycosidic bonds (Gardner, Oporto, Mills, Said, & Samir, 2008). Cellulose molecules are linear in nature and are aggregated through van der Waals forces, intra- and intermolecular hydrogen bonds. The reactive sites in the cellulose are

the three-hydroxyl groups which are also widely responsible for metal nanoparticles bonding characteristics (Gardner et al., 2008).

Silver, inherently possessing antibacterial properties, has been used to accelerate healing of skin wounds (Tian et al., 2007; Maneerung, Tokura, & Rujiravanit, 2008) and also for treating a variety of diseases including pleurodesis and cauterisation. Few researchers have reported on the possible pro-healing properties of silver (Wright, Lam, Buret, Olson, & Burrell, 2002). Recently, silver nanoparticles have been demonstrated to exhibit cytoprotective activities toward HIV-1-infected cells (Sun et al., 2005). The acceleration of delayed wound healing and faster diabetic wound healing (Tian et al., 2007; Mishra, Kumar, & Tripathi, 2008) are additional characteristics of silver nanoparticles (AgNPs) as reported by Tian et al. (2007) and Mishra et al. (2008).

Silver nanoparticles produced by chemical reducing agents are usually associated with environmental toxicity or biological hazards. Therefore, the development of AgNPs based on natural occurring carbohydrates is considered to be one of the most appropriate methods, for obvious environmental reasons. In that category, gum acacia (Gum arabic) and guar gum (Guaran), well-known polysaccharides, derived from acacia tree and guar beans respectively, have been used for the formation and stabilization of AgNPs (Abdel-Halim, El-Rafie, & Al-Deyab Salem, 2011; Vimala, Samba Sivudu, Murali Mohan, Sreedhar, & Mohana Raju, 2009). These natural polymers are not only low cost, but also more

\* Corresponding author.

E-mail addresses: [varmaindian@gmail.com](mailto:varmaindian@gmail.com), [prasadac@gmail.com](mailto:prasadac@gmail.com) (K. Varaprasad).

abundant and have excellent emulsifying and surface-active properties (Akhtar, Dickinson, Mazoyer, & Langendorff, 2002; Mikkonen et al., 2009), which are beneficial for designing metal nanoparticles in nanotechnology.

Of late, the incorporation of AgNPs in cotton fibers has received great attention due to their high resistance to microbes. Vigneshwaran, Kumar, Kathe, Vradarajan, and Prasad (2006) have developed the in situ synthesis of silver nanoparticles on cotton fabrics. Perelshtein et al. (2008) developed a sonochemical method for coating of AgNPs, using ultra sound waves. Duran, Marcato, De Souza, Alves, and Esposito (2007) incorporated silver nanoparticles in to cotton fabrics by fungal process. Yu, Teng, Chou, and Yang (2003) also reported the incorporation of silver nanoparticles into ultrafine fibers by electro spinning.

In the present investigation an efficient, non-toxic, durable and cost effective antimicrobial cellulose fiber with increased applications in medical field have been developed. The key feature of this method was, synthetic reducing agents was completely avoided by employing a green process where naturally available carbohydrates: GA (composed of glycoproteins, arabinose and ribose) and GG (composed of galactose and mannose) were used for the reduction of silver ions to silver nanoparticles. The developed AgNPs were incorporated into cellulose fibers to use as antibacterial finishings. The advantages of the green process are: (a) there is no need to use extra reducing agent, (b) the process can be conducted at ambient temperature of 27 °C and (c) environmentally friendly process.

## 2. Experimental

### 2.1. Materials

Gum acacia powder (GA), gaur gum powder (GG) and silver nitrate ( $\text{AgNO}_3$ ) were purchased from S.D. Fine-Chem Ltd. (Mumbai, India) and used as received without further purification. Cellulose cotton fibers (1 mm thickness) were purchased from SIMCO thread mills (Salem, Chennai, India). Twice distilled water was used in all the experiments.

### 2.2. Preparation of polymer Ag-nanoparticles (poly-AgNPs) solutions

Initially, 100 ml of 0.3%, 0.5% and 0.7% (w/v) GA and GG solutions were prepared separately by stirring respective amounts of GA and GG (gm) in distilled water at 300 rpm for 24 h in an orbital shaking incubator, maintained at ambient temperature. Later, 5 ml of 0.588 mM of  $\text{AgNO}_3$  solution was introduced in to each of the above solutions and stirred at 300 rpm for 80 h by maintaining constant temperature. The natural polymers, GA and GG reduce the  $\text{Ag}^+$  ions of  $\text{AgNO}_3$  present in GA and GG solutions to  $\text{Ag}^0$  nanoparticles to form poly-AgNPs solutions of GA and GG respectively.

### 2.3. Preparation of cellulose–silver nanocomposite fibers (CSNCFs)

CSNCFs were produced by rotating the pre-weighed and washed cellulose fibers (5 g) immersed in the poly-AgNPs solutions in an orbital shaking incubator at 300 rpm for 24 h at an ambient temperature. Rotation allows the AgNPs to be impregnated in the cellulose fibers. Finally, the CSNCFs developed were taken out, dried and kept in a dessicator prior to characterization. Different CSNCFs, having various formulations, were developed from the various concentrations (0.3%, 0.5% and 0.7%) of GA and GG.

### 2.4. Characterization

Formation of AgNPs was monitored for all the poly-AgNPs solutions up to 80 h, using UV–vis spectrophotometer (Elico co, Hyderabad, India). Fourier transform infrared (FTIR) measurement was done using Perkin Elmer (Model Impact 410, Wisconsin, MI, USA) spectrophotometer to determine the shifting of functional groups present in pure GA and GG solutions and in the various poly-AgNP solutions. Thermal properties were determined from the thermogravimetric analysis (TGA) data, using SDT Q 600 thermal analyzer (T.A. Instruments-water LLC, Newcastle, DE, USA), at a heating rate of 20 °C/min and passing nitrogen gas at a flow rate of 100 ml/min. Tensile (tensile strength, modulus and % elongation-at-break) properties were determined using INSTRON 3369 Universal Testing Machine (Buckinghamshire, England), set at a crosshead speed of 5 mm/min and at 23 °C. The sample fibers were cut into 1 mm × 100 mm and mechanical properties were studied using 10 kg load cell by maintaining a gauge length of 50 mm. In each case, four samples were analyzed and the average value was reported. Scanning electron microscope–EDS analysis of cellulose fiber and CSNCFs were performed using a JEOL JEM-7500F (Tokyo, Japan) operated at an accelerating voltage of 15 V. All (SEM-EDS) samples were carbon coated, prior to examination with a field emission scanning electron microscope. Transmission electron microscope (TEM) (JEM-1200EX, JEOL, Tokyo, Japan), was used for the morphological observation. TEM sample was prepared by dispersing two to three drops of (1 mg/1 ml) polymer–silver nanoparticles solution on a 3 mm copper grid and dried at ambient temperature.

### 2.5. Antibacterial activity

The antibacterial activity was tested for all CSNCFs, following inhibition zone method by taking *Escherichia coli* as the model bacteria, using modified agar diffusion assay (disc test) maintained at 37 °C for 1 day as the incubation period. The required nutrient agar medium was prepared by mixing peptone (5.0 g), beef extract (3.0 g) and sodium chloride (5.0 g) in 1000 ml of distilled water and the pH was adjusted to 7.0. Finally, agar (15.0 g) was added to the solution. Sterilization of agar medium was done in a conical flask at a pressure of 6.8 kg (15 lbs) for 30 min. This medium was transferred into sterilized petri dishes in a laminar air flow chamber (Microfilt Laminar Flow Ultra Clean Air Unit, Mumbai, India). After solidification of the media, *E. coli* (50  $\mu\text{l}$ ) culture was spread on the solid surface of the media. Over this inoculated petri dish, small pieces of AgNPs cellulose fibers and pure cellulose fiber (C) were distributed and incubated for 2 days at 37 °C in an incubation chamber. After this period, the inhibition zones observed were photographed.

## 3. Results and discussion

Development of CSNCFs involves the initial synthesis of AgNPs followed by impregnation of the AgNPs into cellulose fibers. The current approach involves the use of 0.3, 0.5 and 0.7% (w/v) GA and GG solutions as reduction media for the preparation of AgNPs from 0.588 mM  $\text{AgNO}_3$ . The conversion of  $\text{Ag}^+$  ions into silver nanoparticles was due to the reduction action of functional groups present in GA and GG (Dorjnamjin, Ariuna, & Shim, 2008), where the pendent hydroxyl groups of GA and GG were assumed to be actively involved in the reduction process. Further, the high molecular chains present in GA and GG provide stabilization for the formed AgNPs. The impregnation of AgNPs in to the cellulose fibers was done by immersing and rotating the cellulose fibers in the poly-AgNPs solutions of GA and GG at 300 rpm for 24 h at ambient

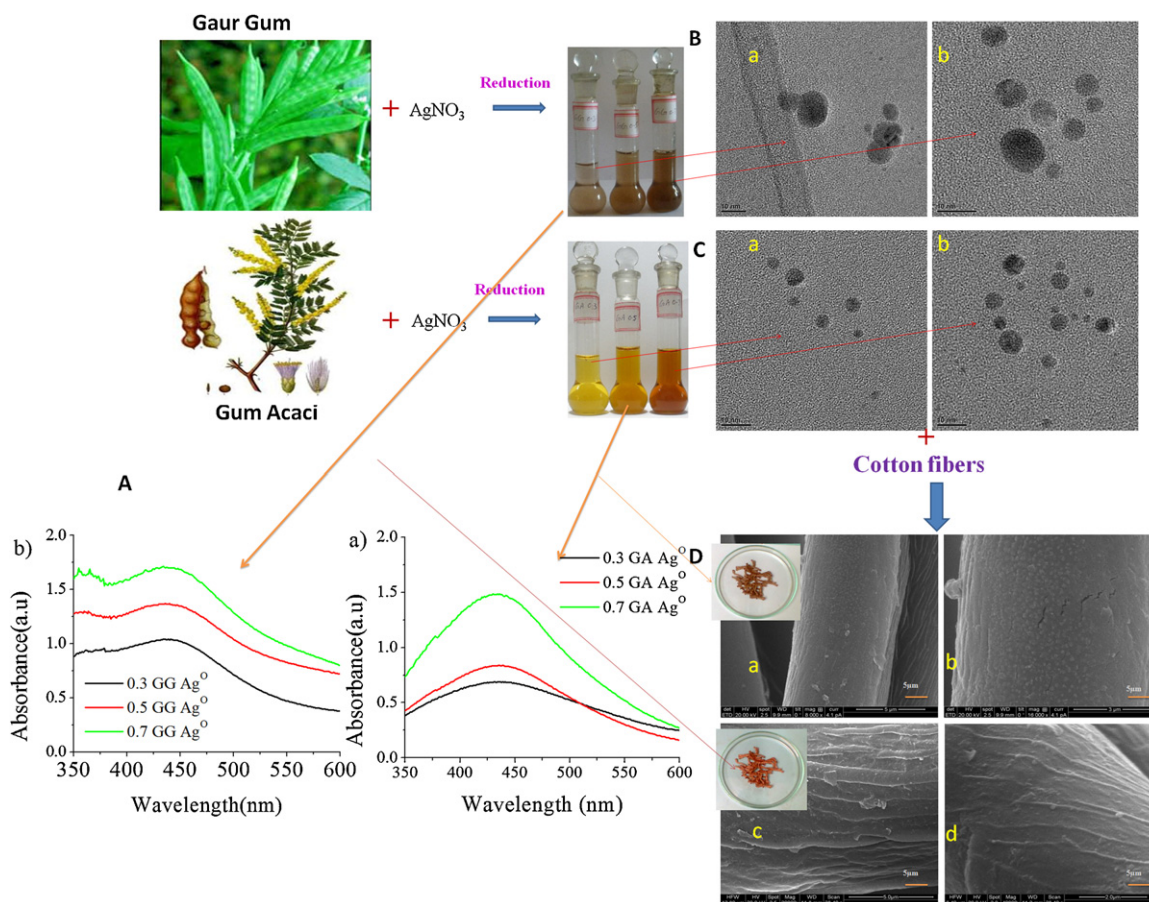


**Fig. 1.** Schematic diagram of formation of cellulose–polymer silver nanocomposites fibers: (A) UV–Visible spectra of (a) GA–AgNPs solution and (b) GG–AgNPs solution; (B) TEM image of (a) GG 0.3% GG–AgNPs solution and (b) 0.7% GG–AgNPs solution; (C) TEM image of (a) 0.3% GA–AgNPs solution and (b) 0.7% GA–AgNPs solution; (D) SEM images of (a) 0.3% GA CSNCF, (b) 0.7% GA CSNCF, (c) 0.3% GG CSNCF and (d) 0.7% GG CSNCF.

temperature of  $27^\circ\text{C}$  in the orbital shaking incubator, and subsequently taken out and dried. Silver nanoparticles deposited on the cellulose fibers were considered to be attached due to physical interactions with the surface hydroxyl groups of cellulose (Gardner et al., 2008). The schematic representation of the formation of silver nanoparticles on the cellulose fibers was illustrated in Fig. 1.

Formation of silver nanoparticles was predicted by color change from colorless to ruby red color of poly-AgNPs solutions and was further confirmed from the UV–vis spectra with intense absorbance band exactly between 430 and 450 nm. This was due to surface plasmon excitation vibrations of the silver nanoparticles (Duran et al., 2007; Shankar, Rai, Ahmad, & Sastry, 2004). The UV–vis spectra of the various GA and GG AgNP solutions taken after reduction time of 80 h was shown in Fig. 1A. From the figure, it was clear that increase in the maximum intensity was observed with corresponding increase of GA and GG concentrations. Furthermore, for the same concentration, GG showed high intense peaks than GA. Absorption peaks at 432.51, 434.65, 435.71, 434.74, 437.95 and 443.16 nm were observed for GA 0.3%, GA 0.5%, GA 0.7%, GG 0.3%, GG 0.5% and GG 0.7% respectively. Also for the same concentration, poly-AgNPs solution of GG showed absorption maxima at higher wavelength than poly-AgNPs solution of GA. This red shift indicates either an increase in size or aggregation of AgNP in GG solutions than in GA solutions (Hettiarachchi and Wickramarachchi, 2011). The same can be confirmed by TEM analysis, where the GG–AgNPs were larger in size than GA–AgNPs were seen. The increase in absorption with time, up to 80 h was shown in Fig. 2.

The formation of AgNPs in polymer solutions (GA, GG) was confirmed from TEM analysis. From the shown TEM images (Fig. 1B and C), it was clear that the AgNPs formed were spherical in nature with an average particle size of  $5 \pm 3$  nm in poly-AgNPs solution of GG (Fig. 1B, a and b) and  $4 \pm 2$  nm in poly-AgNPs solution of GA (Fig. 1C, a and b). From TEM analysis, it was concluded that the size of the formed AgNPs was in between 2 and 8 nm, which was about 62% size compacted than earlier work (Ravindra, Murali

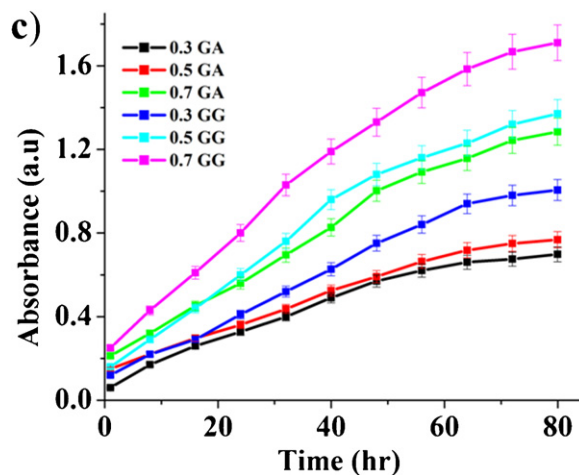


**Fig. 2.** UV absorption and time dependent spectra of polymer–AgNPs (GG, GA) solution.

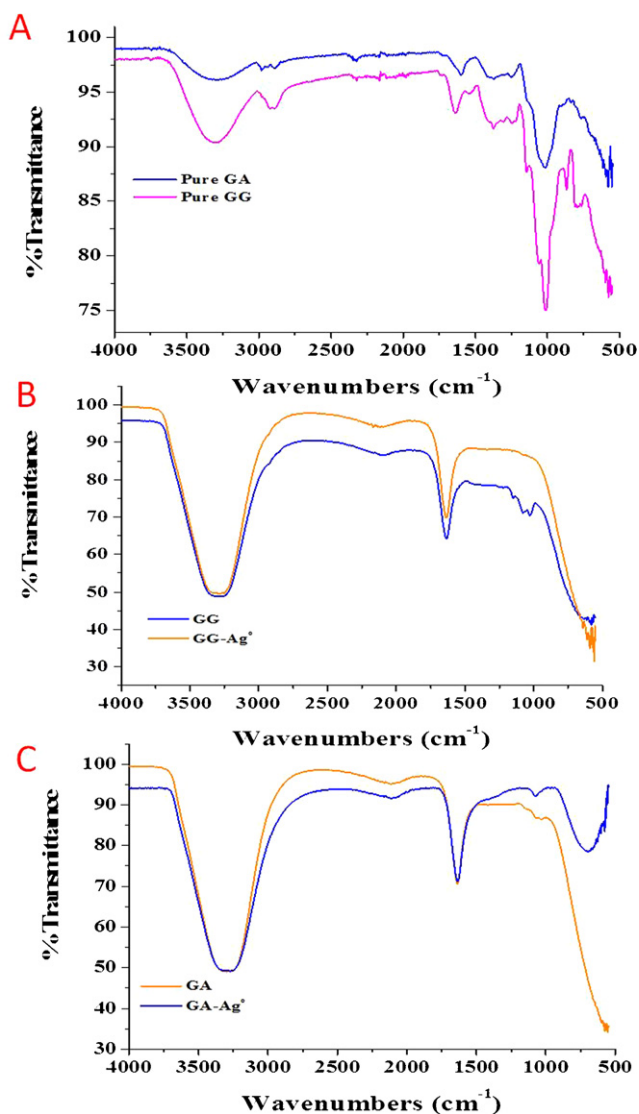


Fig. 3. FTIR spectra of (A) pure GA, GG powder, (B) GG AgNPs (0.5%) solution and (C) GA AgNPs (0.5%) solution.

Mohan, Narayana Reddy, & Mohana Raju, 2010), where the size of AgNPs was around 21 nm. Furthermore, the size of AgNPs in poly-AgNPs solution of GG solutions was larger than size of AgNPs in poly-AgNPs solution of GA solution, which was further supported by UV–vis data where the surface plasmon resonance of the formed AgNPs from GG reduction were observed at higher wave length (red shift) than from GA reduction. It was expected that both GA and GG stabilize the AgNPs by well-established chemical bonding between the functional groups (Sreedhar, Keerthi Devi, & Deepthi, 2011; Abdel-Halim et al., 2011). This can be technically concluded, as the aggregation of AgNPs was not found in TEM images, which may be attributed due to the effective passivation of the surfaces and the suppression of the growth of the nanoparticles through strong interactions via the functional molecular groups of GG (–OH) and GA (–OH, –COOH).

The formation of silver nanoparticles inside the polymer network (GA and GG) was also investigated by FTIR analysis. The FTIR spectra of pure GA, pure GG, aqueous solutions of GA, aqueous solution of GG and aqueous polymer/silver nanoparticles ( $\text{Ag}^0/\text{GA}$  and  $\text{Ag}^0/\text{GG}$ ) solutions were recorded, in order to identify the functional groups involved in the synthesis of AgNPs.

GG: The FTIR spectrum of pure GG was presented in Fig. 3. In case of GG, a broad band at  $3304\text{ cm}^{-1}$  due to the presence of –OH stretching was observed, a sharp absorption band located at  $2925\text{ cm}^{-1}$  can be attributed to CH group stretching and a band at  $1635\text{ cm}^{-1}$  (due to the ring stretching) were also observed (Rrath, Subramanian, Sivanandam, & Pradeep, 2001). Other important peaks observed (Fig. 3A) at  $1249$  and  $1012\text{ cm}^{-1}$  were due to the C–O–C stretching from the glycosidic linkages and O–H bending from alcohols (Sharma & Lalita, 2011). A considerable modification can be noticed (Fig. 3B) in the well-defined spectrum of aqueous solution of guar gum and aqueous poly-AgNPs.

GA: The spectrum of GA showed many strong peaks (Fig. 3A) at  $3299$  (OH stretching)  $2976$ ,  $2897$  (asymmetric and symmetric C–H stretching) and  $1602\text{ cm}^{-1}$  (C=O stretching of the carbonyl group, typical of saccharide absorption) (Juby et al., 2012). It was noticed that when acacia molecules anchor to the distilled water and silver nanoparticles surfaces, their functional group frequencies were shifted (Fig. 3C).

Over all, shifting of peaks confirms the encapsulation of AgNPs by GG or GA molecules, providing stabilization for the formed AgNPs (Sreedhar et al., 2011). After the formation of AgNPs was confirmed from ultraviolet–visible (UV–vis), transmission electron microscopy (TEM) and Fourier transforms infrared (FTIR) studies; AgNPs were impregnated in the cellulose fibers. For the impregnated cellulose fibers, effect of polymer-AgNPs on the cellulose fibers was studied and the same was described in the following (SEM-EDS, UTM and TGA) segment of this report.

### 3.1. Scanning electron microscopy–energy dispersive spectroscopy (SEM-EDS) analysis of CSNCFs

To evaluate the dispersion of poly-AgNPs on the cellulose fibers, SEM observations (Figs. 1D and 4) were carried out and the results were compared with pure cellulose fiber (Fig. 4A) and polymer-coated cellulose fibers (Fig. 4B). The images were shown in Figs. 1D and 4C, which demonstrate that the dispersed poly-AgNPs were smaller in size without any aggregations. For a better view, the fibers were scanned at higher magnifications. Overall, the surface topography indicated that poly-AgNPs were intensely deposited on the fibers by the current approach.

EDS spectrum was used to find the type of particles that were absorbed in to the surface of cellulose fibers. Fig. 5A shows the EDS spectrum of pure cellulose fibers and CSNCFs samples. The EDS spectrum of the pure cellulose fibers (Fig. 5A, a) did not show any characteristic peak of silver, while the EDS spectra of CSNCFs (Fig. 5A, b and c) clearly showed the characteristic peak for silver confirming the existence of  $\text{Ag}^0$  element on the CSNCFs surfaces. It was observed that Ag is a major element on the CSNCFs.

### 3.2. Mechanical properties

The tensile stress–strain curves data of CSNCFs fibers of GA, GG and pure cellulose fiber were depicted in Table 1. The data illustrates the mechanical properties such as: maximum stress (Fig. 5B, a), Young's modulus (Fig. 5B, b) and % elongation-at-break (Fig. 5B, c) of all the cellulose fibers. The results indicate that the CSNCFs can be utilized for longer duration of use without any significant damage or breakage.

### 3.3. Thermal properties

To verify the thermal stability of CSNCFs fibers, thermal properties of the fibers were examined by thermogravimetric analysis (TGA). The primary thermograms of CSNCFs of GA and GG with

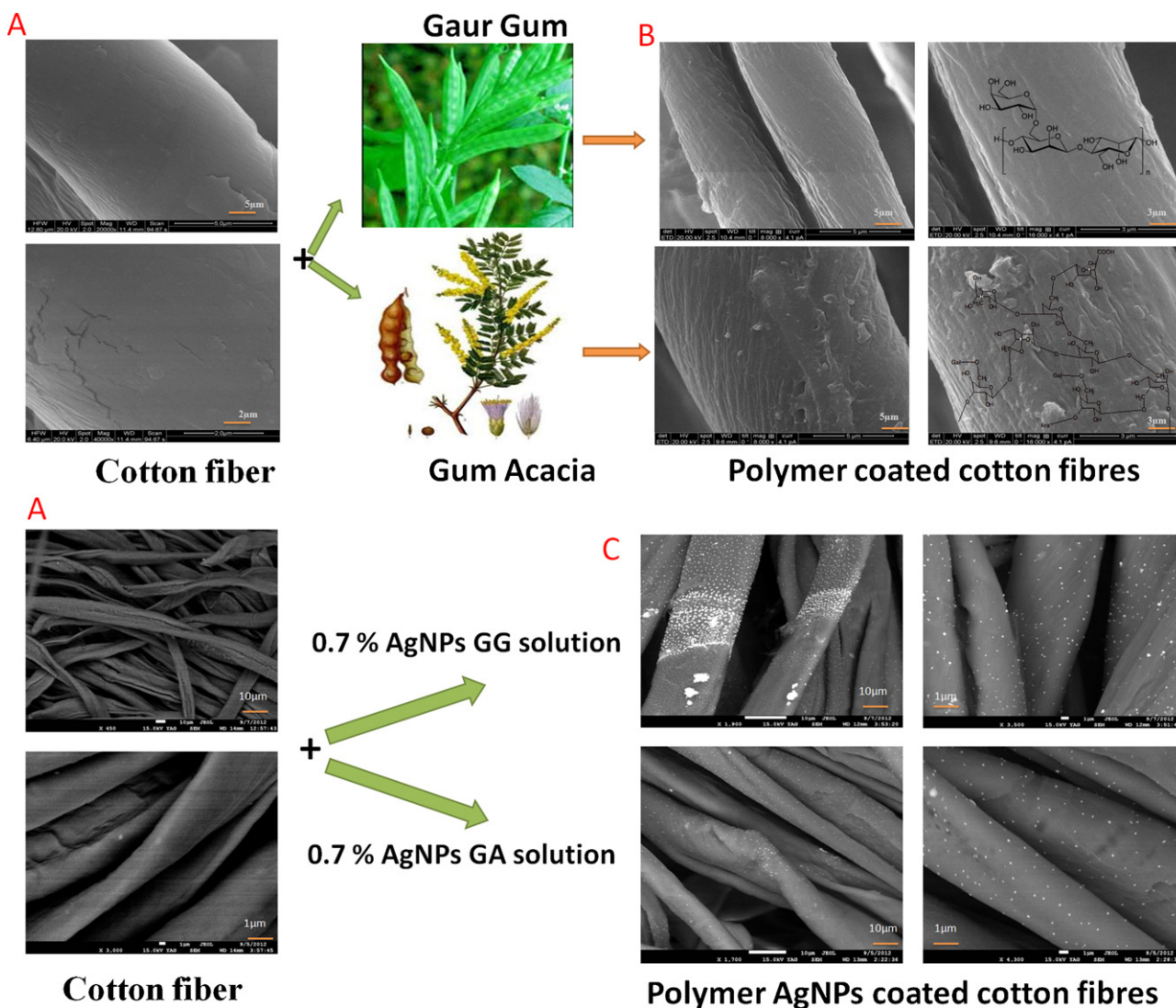


Fig. 4. SEM images of (A) pure cotton cellulose fibers, (B) polymer coated cellulose fibers, and (C) polymer-AgNPs coated cellulose fibers.

Table 1

Mechanical properties of cellulose fibres with polymers and cellulose-silver nanocomposites fibres.

Sample code	Maximum stress (MPa)		Young's modulus (MPa)		Elongation at break (%)	
	Cotton fiber with polymers	Cotton fiber with polymers and Ag <sup>0</sup>	Cotton fiber with polymers	Cotton fiber with polymers and Ag <sup>0</sup>	Cotton fiber with polymers	Cotton fiber with polymers and Ag <sup>0</sup>
0.3 GA	21.14	25.12	176.30	215.12	21.52	21.65
0.7 GA	37.35	39.86	305.45	311.15	22.20	23.15
0.3 GG	14.83	17.30	128.17	154.19	21.15	21.69
0.7 GG	33.64	38.70	274.45	310.27	22.72	22.75

reference to pure cellulose fiber (C) are shown in Fig. 6a and b respectively. The results indicated that, in case of AgNPs-loaded CSNCFs fibers, an initial weight loss at a temperature below 100 °C was observed and this was due to the loss of moisture present on the AgNPs and cotton fibers. Also, the maximum decomposition of all CSNCFs occurred at a slight higher temperature at around 398.68 °C when compared to that of pure cellulose fiber. Thermal studies led to the conclusion that with the increase in the percentage (%) of GA and GG, the stability also increased. This might be due to the rise in nanoparticles number on the cellulose fibres' surface, which occurred due to the strong bonding characteristics developed among AgNPs and cellulose fibers with increase in GA and GG

concentrations. Overall, thermal analysis indicated that the CSNCFs designed were thermally stable.

#### 3.4. Antibacterial properties

AgNPs inherently possess bacteria killing property but more effective action of AgNPs on the bacteria always plays a major role in deciding its well functioning. In the current approach, much smaller synthesis of AgNPs by green process was developed. These smaller AgNPs enter into the bacteria cell more effectively, causing damage to the nuclei and resulting to bacteria death at a faster rate. Also, the smaller AgNPs kill bacteria more effectively

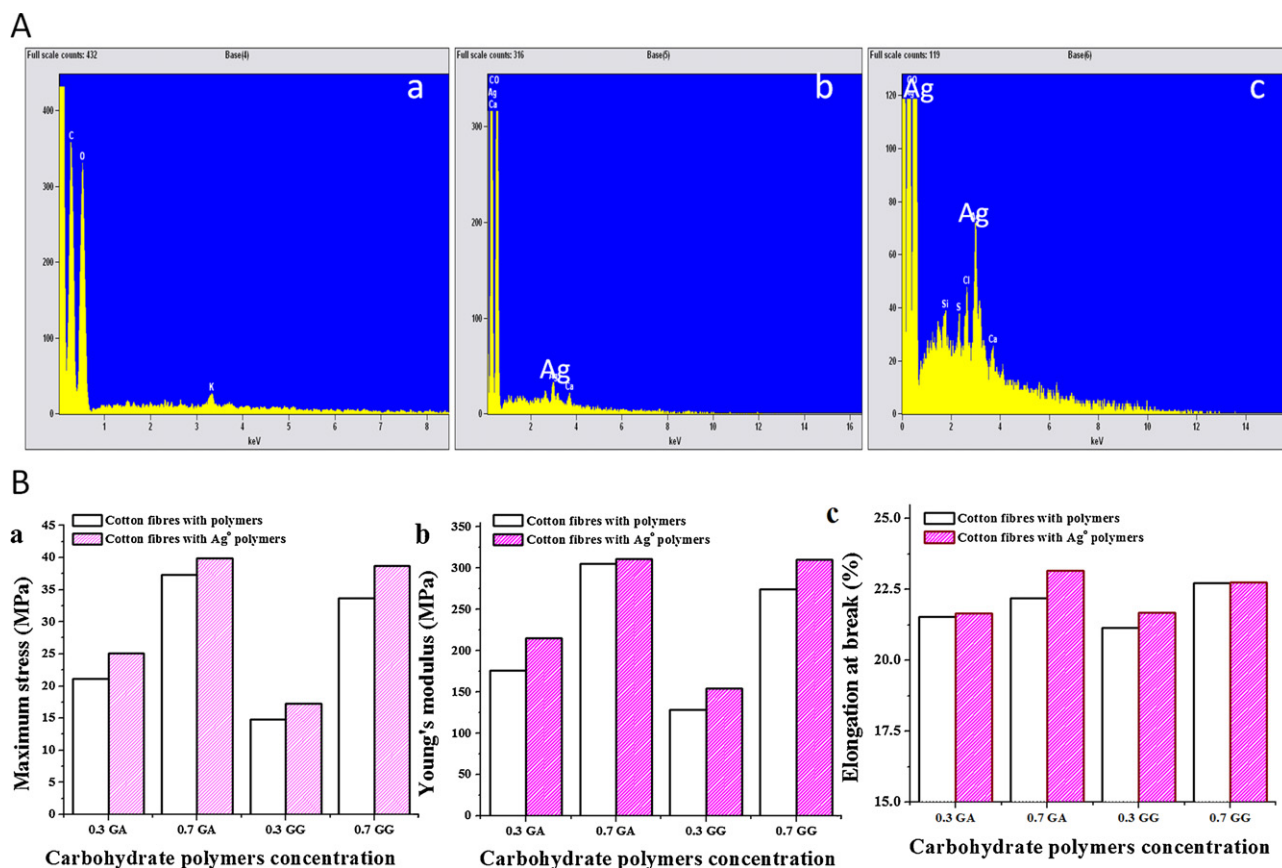


**Fig. 5.** (A) EDS images of (a) pure cellulose fibers, (b) 0.7% GA CSNCF and (c) 0.7% GG CSNCF. (B) Uniaxial stress–strain curves of polymer cellulose fibers and cellulose–silver nanocomposites fibers (a: maximum stress; b: Young's modulus; c: % elongation at break).

than the bigger AgNPs was supported from the investigations of Morones et al. (2005), Varaprasad, Murali Mohan, Vimala, and Mohana Raju (2011), Varaprasad, Vimala, et al. (2011) and Murthy, Murali Mohan, Varaprasad, Sreedhar, and Mohana Raju (2008). The antimicrobial efficacy of the CSNCFs developed from AgNPs was tested against gram negative bacterium *E. coli*. The inhibition zone for all the fibers was found to be higher than 1.7 mm, shown in Fig. 7. According to the Standard Antibacterial test “SNV 195920–1992”, specimens showing more than 1 mm microbial zone inhibition can be considered as good antibacterial agents (Pollini, Russo, Licciulli, Sannino, & Maffezzoli, 2009). Hence, the developed CSNCFs from

the current approach can be considered as good antibacterial agents and effective in killing the microbes. It was also concluded that the developed CSNCFs in the present investigation exhibited higher inhibition zone than earlier reported work of Ravindra et al. (2010). This achievement was because of synthesizing much smaller AgNPs in the current approach when compared with the work of Ravindra et al. (2010). Hence, the improved result. Further, it was noticed that for the same concentration of polymer as reducing media, CSNCFs developed from GG show higher inhibition zone than those of CSNCFs developed from GA, which was evident from Fig. 7.

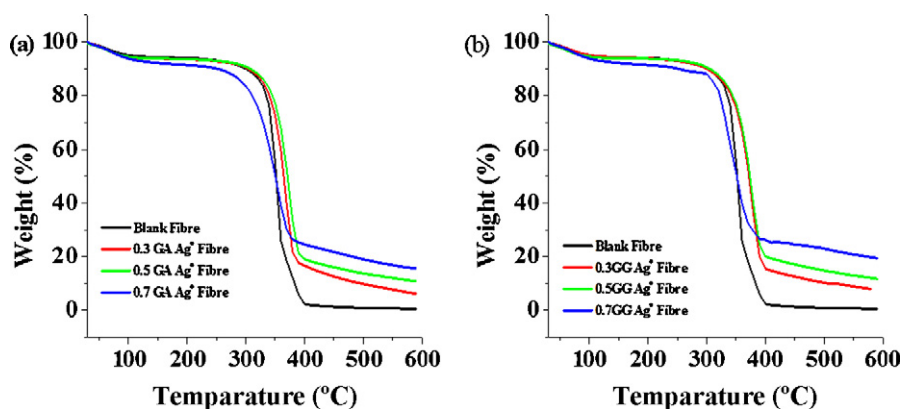


**Fig. 6.** Thermo gravimetric analysis of (a) GA CSNCFs and (b) GG CSNCFs.

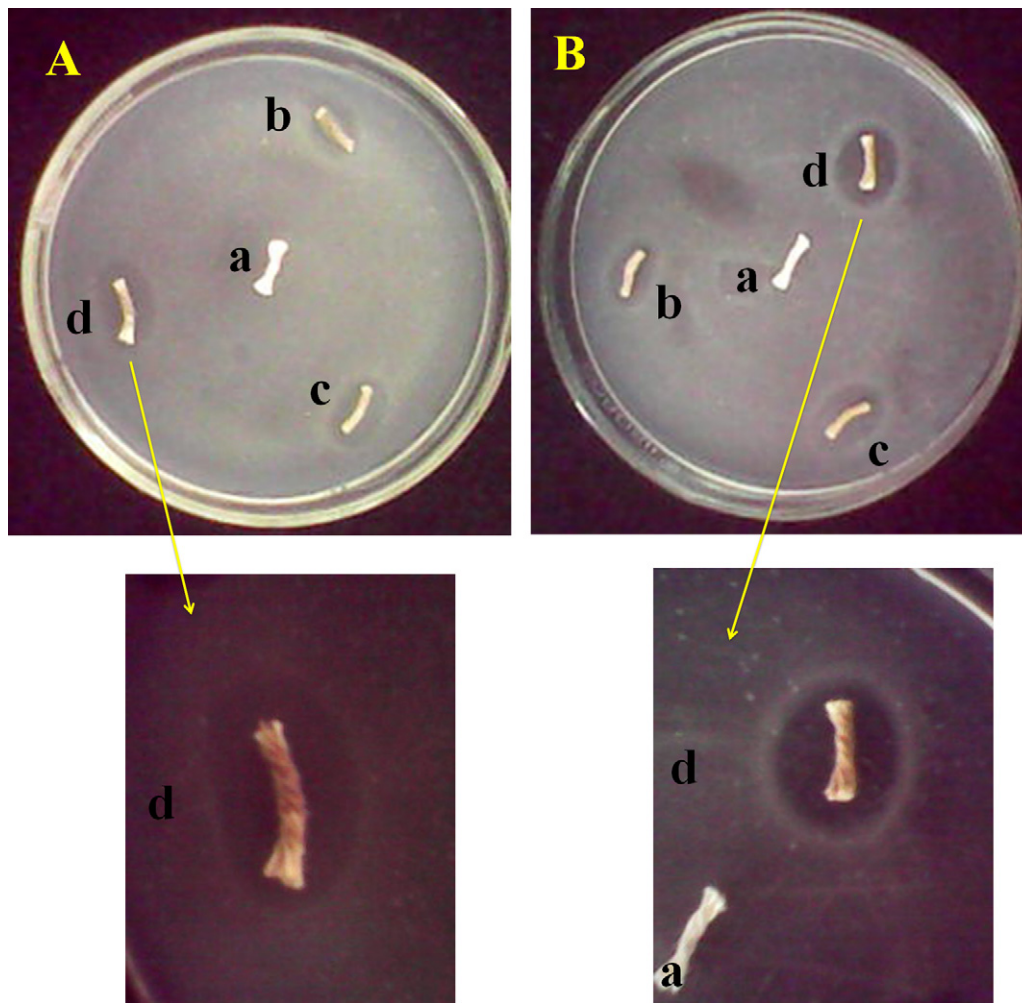


**Fig. 7.** Antibacterial activity of (A) a: GA polymer coated cellulose fibers, b: 0.3% GA CSNCF, c: 0.5% GA CSNCF and d: 0.7% CSNCF on *E. coli*; (B) a: GG polymer coated cellulose fibers, b: 0.3% GG CSNCF, c: 0.5% GG CSNCF and d: 0.7% GG CSNCF on *E. coli*.

#### 4. Conclusion

Cellulose–silver nanocomposites fibers with excellent antimicrobial properties were successfully developed from a green process where  $\text{AgNO}_3$  was reduced with natural carbohydrates, GA and GG. The composites were characterized by spectral, thermal and electron microscopy techniques. The results showed that the silver nanoparticles were greatly dispersed in the cellulose matrix with strong interaction between the cellulose and polymer/silver particles. The CSNCFs exhibited good antibacterial activity against *E. coli*. Therefore, it was concluded that the AgNPs composite cellulose fibers developed can be suggested for their utilization as effective tissue scaffolding for burn/wound treatments. The fibers alone can be used as higher durable antibacterial finishings in textiles industries and also as potential surgical fabrics in the medical fields.

#### Acknowledgements

The authors wish to acknowledge the Department of Science & Technology (DST, India) and Ministry of Science & Technology for providing financial assistance through Innovation In Science Pursuit for Inspired Research (INSPIRE) programme.

#### References

Abdel-Halim, E. S., El-Rafie, M. H., & Al-Deyab Salem, S. (2011). Polyacrylamide/guar gum graft copolymer for preparation of silver nanoparticles. *Carbohydrate Polymers*, 85, 692–697.

- Akhtar, M., Dickinson, E., Mazoyer, J., & Langendorff, V. (2002). Emulsion stabilizing properties of depolymerized pectin. *Food Hydrocolloids*, 16, 249–256.
- Dorjnamjin, D., Ariuna, M., & Shim, Y. K. (2008). Synthesis of silver nanoparticles using hydroxyl functionalized ionic liquids and their antimicrobial activity. *International Journal of Molecular Sciences*, 9, 807–820.
- Duran, N., Marcato, P., De Souza, G. I. H., Alves, O. L., & Esposito, E. (2007). Antibacterial effect of silver nanoparticles produced by fungal process on textile fabrics and their effluent treatment. *Journal of Biomedical Nanotechnology*, 3, 203–208.
- Gardner, D. J., Oporto, G. S., Mills, R., Said, M. A., & Samir, A. (2008). Adhesion and surface issues in cellulose and nanocellulose. *Journal of Adhesion Science and Technology*, 22, 545–567.
- Hettiarachchi, M. A., & Wickramarachchi, P. A. S. R. (2011). Synthesis of chitosan stabilized silver nanoparticles using gamma ray irradiation and characterization. *Journal of Science of the University of Kelaniya Sri Lanka*, 6, 65–75.
- Juby, K. A., Dwivedi, C., Kumar, M., Swathi, K., Misra, H. S., & Bajaj, P. N. (2012). Silver nanoparticle-loaded PVA/gum acacia hydrogel: Synthesis, characterization and antibacterial study. *Carbohydrate Polymers*, 89, 906–913.
- Maneering, T., Tokura, S., & Rujiravanit, R. (2008). Impregnation of silver nanoparticles into bacterial cellulose for antimicrobial wound dressing. *Carbohydrate Polymers*, 72, 43–51.
- Mikkonen, K. S., Tenkanen, M., Cooke, P., Xu, C., Rita, H., Willfo, S., et al. (2009). Mannans as stabilizers of oil-in-water beverage emulsions. *LWT – Food Science and Technology*, 42, 849–855.
- Mishra, M., Kumar, H., & Tripathi, K. (2008). Diabetic delayed wound healing and the role of silver nanoparticles. *Digest Journal of Nanomaterials and Biostructures*, 2008, 49–54.
- Morones, J. R., Elechiguerra, J. L., Camacho, A., Holt, K., Kouri, J. B., Tapia, J., et al. (2005). The bactericidal effect of silver nanoparticles. *Nanotechnology*, 16, 2346–2353.
- Murthy, P. S. K., Murali Mohan, Y., Varaprasad, K., Sreedhar, B., & Mohana Raju, K. (2008). First successful design of semi-IPN hydrogel–silver nanocomposites: A facile approach for antibacterial application. *Journal of Colloid and Interface Science*, 318, 217–224.



- Mucha, H., Hoter, D., & Swerev, M. (2002). Antimicrobial finishes and modifications. *Melli and International*, 8, 148–151.
- Perelshtein, I., Applerot, G., Perkas, N., Guibert, G., Mikhailov, S., & Gedanken, A. (2008). Sonochemical coating of silver nanoparticles on textile fabrics (nylon, polyester and cotton) and their antibacterial activity. *Nanotechnology*, 19, 1–6.
- Pollini, M., Russo, M., Licciulli, A., Sannino, A., & Maffezzoli, A. (2009). Characterization of antibacterial silver coated yarns. *Journal of Materials Science: Materials in Medicine*, 20, 2361–2366.
- Ravindra, S., Murali Mohan, Y., Narayana Reddy, N., & Mohana Raju, K. (2010). Fabrication of antibacterial cotton fibres loaded with silver nanoparticles via Green approach. *Colloids and Surfaces A: Physicochemical Engineering Aspects*, 367, 31–40.
- Rrath, R. K., Subramanian, S., Sivanandam, V., & Pradeep, T. (2001). Studies on the interaction of guar gum with chalcocopyrite. *Canadian Metallurgical Quarterly*, 40, 01–12.
- Shankar, S. S., Rai, A., Ahmad, A., & Sastry, M. (2004). Rapid synthesis of Au, Ag, and bimetallic Au core–Ag shell nanoparticles using Neem (*Azadirachta indica*) leaf broth. *Journal of Colloid and Interface Science*, 275, 496–502.
- Sharma, R. K., & Lalita. (2011). Synthesis and characterization of graft copolymers of N-vinyl-2-pyrrolidone onto guar gum for sorption of Fe<sup>2+</sup> and Cr<sup>6+</sup> ions. *Carbohydrate Polymers*, 83, 1929–1936.
- Sreedhar, B., Keerthi Devi, D., & Deepthi, Y. (2011). Selective hydrogenation of nitroarenes using gum acacia supported Pt colloid an effective reusable catalyst in aqueous medium. *Catalysis Communications*, 12, 1009–1014.
- Sun, R. W., Chen, R., Chung, N. P., Ho, C. M., Lin, C. L., & Che, C. M. (2005). Silver nanoparticles fabricated in Hepes buffer exhibit cytoprotective activities toward HIV-1 infected cells. *Chemical Communications (Cambridge)*, 40, 5059–5061.
- Tian, J., Wong, K. K., Ho, C. M., Lok, C. N., Yu, W. Y., Che, C. M., et al. (2007). Topical delivery of silver nanoparticles promotes wound healing. *ChemMedChem*, 2, 129–136.
- Vaideki, K., Jayakumar, S., Rajendran, R., & Thilagavathi, G. (2008). Investigation on the effect of RF air plasma and neem leaf extract treatment on the surface modification and antimicrobial activity of cotton fabric. *Applied Surface Science*, 22, 2472–2478.
- Varaprasad, K., Murali Mohan, Y., Vimala, K., & Mohana Raju, K. (2011). Synthesis and characterization of hydrogel-silver nanoparticle-curcumin composites for wound dressing and antibacterial application. *Journal of Applied Polymer Science*, 121784–121796.
- Varaprasad, K., Vimala, K., Ravindra, S., Narayana Reddy, N., Venkata Subba Reddy, G., & Mohana Raju, K. (2011). Fabrication of silver nanocomposite films impregnated with curcumin for superior antibacterial applications. *Journal of Materials Science: Materials in Medicine*, 22, 1863–1872.
- Vigneshwaran, N., Kumar, S., Kathe, A. A., Vradarajan, P. V., & Prasad, V. (2006). Functional finishing of cotton fabrics using zinc oxide–soluble starch nanocomposites. *Nanotechnology*, 17, 5087–5095.
- Vimala, K., Samba Sivudu, K., Murali Mohan, Y., Sreedhar, B., & Mohana Raju, K. (2009). Controlled silver nanoparticles synthesis in semi-hydrogel networks of poly (acrylamide) and carbohydrates: A rational methodology for antibacterial application. *Carbohydrate Polymers*, 75, 463–471.
- Wright, J. B., Lam, K., Buret, A. G., Olson, M. E., & Burrell, R. E. (2002). Early healing events in a porcine model of contaminated wounds: Effects of nanocrystalline silver on matrix metalloproteinases, cell apoptosis, and healing. *Wound Repair and Regeneration*, 10, 141–151.
- Yu, D. G., Teng, M. Y., Chou, W. L., & Yang, M. C. (2003). Characterization and inhibitor effect of antibacterial PAN-based hollow fibre loaded with silver nitrate. *Journal of Membrane Science*, 225, 115–123.